Interaction of negatively and positively capped gold nanoparticle with different lipid model membranes.

Alan J. Sheridan,* Katherine C. Thompson,* and Jonathan M. Slater

Department of Biological Sciences and Institute of Structural and Molecular Biology, Birkbeck College, University of London, Malet Street, London WC1E 7HX, U.K.

E-mail: a.sheridan@mail.cryst.bbk.ac.uk; k.thompson@mail.cryst.bbk.ac.uk

Highlights

- Examined positively and negatively capped gold nanoparticles interacting with different lipid bilayers and monolayers using Langmuir trough and quartz crystal microbalance.
- Interaction of negatively charged particles with Zwitterionic monolayers greater than with negatively charged lipid monolayers, whilst positively charged particles interacted more with an anionic monolyaer.
- Citrate capped gold nanoparticles showed only very limited interaction with a lipid bilayer below T_m of the bilayer, but large interaction above T_m.

Abstract

The use of functionalised gold nanoparticles in biomedical applications is expanding. Here we explore the interaction of gold nanoparticles with lipid membranes using

readily available equipment and basic techniques to explore how the charge on the nanoparticles, and the nature of the lipid, influences the interaction. Gold nanoparticles were synthesised with two different surface functionalisations, negatively charged citrate groups and positively charged cetyltrimethylammonium groups from CTAB, to determine how surface charge affects the interaction of the nanoparticles with the Zwitterionic lipid POPC and the anionic lipid POPG. It was observed that the surface pressure/area isotherms of POPG monolayers on exposure to citrate capped nanoparticles were not shifted to higher molecular areas as much as those of POPC, suggesting that the anionic headgroups of the POPG lipid repel the anionic surface charge of the citrate capped nanoparticles to some extent limiting inclusion. In contrast, the surface pressure/area isotherms of the POPG monolayers exposed to CTAB capped nanoparticles are shifted to higher molecular areas more than for the POPC monolayers. The interaction of anionic nanoparticles with lipid bilayers was measured by the mass change of the bilayer deposited on the surface of a quartz crystal microbalance (QCM) exposed to nanoparticles in an aqueous phase flow. The QCM frequency changes show that bilayers of unsaturated phosophocholine lipids readily took up particles, whereas for the saturated lipid DPPC significant uptake was only observed when the bilayer was warmed to above its gel-to-fluid transition temperature, T_m. This is possibly due to an increase in the molecular mobility and bilayer bending modulus, κ, of the bilayer.

Graphical abstract

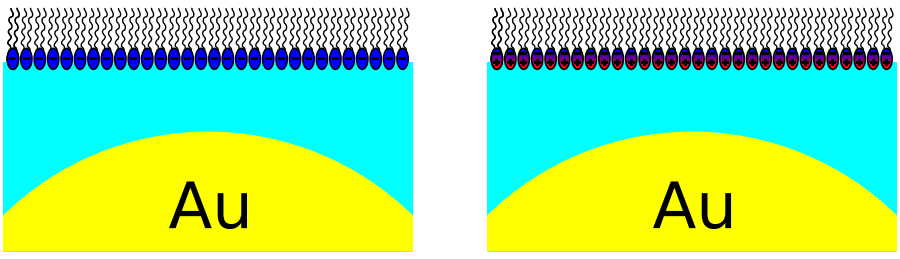

Keywords

Gold nanoparticles; Lipid membranes, Bilayers and Monolayers; Quartz Crystal Microbalance; Langmuir trough.

Introduction

There is a great deal of interest in the use of manufactured nanoparticles, notably gold nanoparticles, as novel drug carriers and as therapeutic and/or diagnostic agents for various illnesses.[1] As such, understanding and control over the interaction between gold nanoparticles and biological mambranes is very important for the development of these carriers for different biomedical applications. When considering the interaction of a nanoparticle with a cell membrane, in the absence of a specific receptor on the cell surface, the interaction will be between the surface of the nanoparticle and the lipid membrane and, initially, with the lipid head groups.

For a detailed review of the issue the reader is directed to the work of Contini *et al.*[2] Four scenarios can readily be imagined: (i) the particle crosses over the membrane completely, (ii) the particle becomes embedded in the core of the membrane (within the lipid tail region), (iii) the particle embeds in the outer lipid head regions of the membrane to some extent, causing local membrane deformation and (iv) the particle does not interact significantly with the membrane. The likelihood of each of these scenarios occurring depends on the surface composition and physical properties of the gold nanoparticle and on the composition and physical properties of the membrane. The interaction of nanoparticles with lipid membranes can therefore be expected to depend upon the nature of the lipid tail region, particularly its thickness and fluidity, the packing of the head group region, the charge (or lack of) of the lipid head group, and, at least, the size, shape, hydrophilicity (or lipophilicity) and surface charge of the nanoparticles. Natural membranes are composed of a wide range of different lipid types. Zwitterionic phosphocholine lipids are a major part of mammalian

membranes whereas they are uncommon in bacteria. Similarly, anionic phosphoglycerol lipids are common in bacteria but much less so in mammalian membranes.[3]

In this work we have considered the interaction of gold nanoparticles with Zwitterionic and anionic liquid-expanded lipid monolayers to explore how the charge on the lipid head group influences the interaction with the particles. Two particle types were used: citrate capped gold nanoparticles of 18 and 9 nm diameter, which carry a negative surface charge, and cetyltrimethylammonium (CTAB) capped nanoparticles of 17 nm, which carry a positive surface charge.

Citrate capped gold nanoparticles have been used by others studying lipid membrane/ nanoparticle interactions. Bakshi *et al.* used captive bubble tensiometry to show that the presence of citrate capped gold nanoparticles increased the minimum surface tension obtained by films of two lipids found in lung surfactant: dipalmitoylphosphatidylcholine (DPPC) and palmitoyloleoylphosphatidylglycerol (POPG), thus reducing the effectiveness of the membrane.[4] Bailey *et al.* performed experiments using low concentrations of citrate capped gold nanoparticles and supported fluid lipid bilayers and found no evidence of particle uptake into the bilayer.[5] Contini *et al.* looked at the interaction of different sizes of citrate capped gold nanoparticles with lipid vesicles.[2] The authors report different regimes: when the ratio of the lipid vesicle to nanoparticle size is large the particles tend to aggregate on the membrane and become partially wrapped, at small ratios less interaction is observed, attributed to the increased energetic cost of bending large sections of the membrane whereas at intermediate ratios the particles embed to a measurable extent in the membrane. The supported lipid bilayers studied in the current work are most similar to the situation of a large lipid vesicle to nanoparticle size, and thus we would expected the particles to be taken up by the membrane and partially wrapped by it.

Guzmán *et al.* investigated the effect of silica nanoparticles on monolayers of DPPC and palmitic acid (PA) in various mixtures using a Lanmuir-Blodgett trough and Brewster Angle Microscopy (BAM). They found that incorporation of the nanoparticles into the monolayer

affected the phase behaviour of the layer as well as resulting in a reduction in the collapse pressure of the DPPC-PA monolayer. They suggest that the incorporation of the silica nanoparticles into the monolayer is assisted by the nanoparticles developing a layer of lipid on their surfaces, thus making them more hydrophobic.[6]

Guzmán *et al.* also studied the collapse surface pressure, Π_c, of DPPC monolayers when exposed to carbon black (CB) and silicon dioxide, SiO_2, nanoparticles.[7] They observed a higher decrease in Π_c for the DPPC monolayers when exposed to SiO_2 nanoparticles compared to CB nanoparticles. This they attributed to steric hinderence due to the spherical-like aggregation of the CB nanoparticles as opposed to the chain-like aggregation of the SiO_2 nanoparticles. Their work demonstrated the possible affect of surface chemistry of nanoparticles on their interaction with lipid monolayers: the silanol groups present on the surface of the SiO_2 nanoparticles may introduce a repulsive electrostatic interaction resulting in dispersion of the SiO_2 particles within the DPPC monolayers. The study of Guzmán *et al.* was focused on the electrotatic interaction of the nanoparticles with each other due to their surface chemistry and the consequential affect this would have on their interaction with DPPC lipids and not on the possible electrostatic interaction of the nanoparticles with the lipid molocules themselves.

Guzmán *et al.* revisited their research into the effect of silica nanoparticles on lipid monolayers, but this time they studied mixed layers of DPPC and 1,2-Dioleoyl-sn-glycero-3-phosphocholine (DOPC).[8] Again, they measured the π—A isotherms for the monolayers, but also used BAM and Atomic Force Microscopy (AFM), to obtain morphological information on the monolayers. Without the influence of the silica nanoparticles the isotherm of the mixed DPPC/DOPC monolayer falls between those of the pure lipids with regards to the π—A isotherm values and collapse pressures. With the inclusion of silica nanoparticles at 1 wt %, AFM showed the existence of irregular domains, making the monolayer less homogeneous. AFM also displayed areas with heights similar to the size of the nanoparticles.

Further studies by Orsi *et al.* using fluorescently labeled DPPC molecules showed that

silica nanoparticles incorporated into a DPPC monolayer form a mixed phase consisting of round islands of pure DPPC domains. These domains resist the incorporation of the silica nanoparticles due to their close-packed structure resulting in a stable mixed matrix of nanoparticle-incorported lipid surrounding pure DPPC domains.[9]

In other work, etalGuzmán studied the interaction of silica nanoparticles on monolayers of cholesterol and cholesterol/DPPC mixtures as well as lipid mixtures of DPPC, DOPC and cholesterol.[10,11] They observed that silica nanoparticles in the sub-phase of a Languir-Blodgett trough incorporated into the monolayer due to interactions of the nanoparticles with the lipid molecules making them partially hydrophobic. They suggest that interaction between the cholesterol and nanoparticle is driven by hydrogen bonding between the silanol groups on the surface of the nanoparticles and the hydroxyl group of the cholesterol. The incorporation of the nanoparticles into the monolayer resulted in the surface pressure starting to increase at lower compression and the isotherm being shifted to higher areas; that is, nanoparticles incorporated at the interface induce a steric hindrance to compression leading to the increase of π at areas per molecule higher than those of pure cholesterol.

Van Lehn *et al.* studied the interaction of anionic gold nanoparticles coated with a monolayer of a hydrophilic, 11-mercaptoundecane sultanate, and hydrophobic, 1-octanethiol, ligands in various ratios with DOPC vesicles.[12] It was shown that increasing the ratio of hydrophobic lipids led to an increase in the hydrophobic surface area of the monolayer which increased the level of penetration of the nanoparticle into the bilayer. Fusion of the particles with the bilayer was only favourable below a critical size, which will depend on the composition of the monolayer coating the particle and on the lipid bilayer composition.[13]

Pfeiffer *et al.* have explored the interaction of positively charged 4 nm gold nanoparticles with bilayers of palmitoyloleoylphophatidylcholine (POPC) and POPG mixtures. They found that the particles adhered irreversibly to the lipid bilayer and molecular dynamics simulations suggested that the POPG lipids in the mixed bilayer interacted more with the nanoparticles than the POPC lipids.[14]

The positively charged particles used in this work were capped with CTAB and thus had a positive surface charge and a hydrophobic tail region surrounding the gold core. Particles of this type (gold core with a surfactant coating) have been studied by others. Schaeublin *et al.* found that cationic nanoparticles have been shown to disrupt cell membranes and that the level of disruption has been shown to be related to the size and charge of the nanoparticle.[15]

Torrano *et al.* found that the in plane elasticity of negatively charged DPPG monolayers increased with adsorption of cationic gold nanoparticles funtionalized with poly(allylamine hydrochloride) as opposed to citrate capped gold nanoparticles whereas the opposite effect was observed for zwitterionic DPPC monolayers.[16] Hu *et al.* used pulsed laser ablation produced gold nanoparticles functionalised with carboxyl- or amine- groups on 1,2-distearoyl-sn-glycero-3-phosphocholine (DSPC) bilayers. They found that higher surface coverage of carboxyl functional groups on gold nanoparticles tended to induce lipid 'flip-flop' between the leaflets of the bilayer at a higher rate than for amine-functionalised nanoparticles.[17]

Canepa *et al.* studied the penetration of sub-6 nm gold nanoparticles funtionalised with anionic 11-mercapto-1-undecanesulfonate or cationic (11-mercaptoundecyl)-N,N,N-trimethylammonium into model neutral lipid membranes composed of zwitterionic POPC. They found that both the anionic and cationic nanoparticles could penetrate through the membranes without inducing significant membrane damage.[18]

The study of nanoparticles and their interactions with biological membranes is made more difficult by the fact that observations generally require nanoscale measurements with not-readily available techniques such as X-ray or neutron reflectivity or computer intensive molecular dynamics simulations. A goal of this study is to investigate the potential value of using simple and readily available equipment and established experimental techniques in the study of nanoparticles and their interactions with biological interfaces.

In this study, a Langmuir-Blodgett trough was used to study the interaction of functionalised nanoparticles with lipid headgroups. Both classes of functionalised nanoparticles were exposed to lipid monolayers deposited on a Langmuir-Blodgett trough to measure any pos-

sible changes in their surface pressure/area isotherms to determine if the functionalisation affects the interaction of the nanoparticles with lipid membranes.

In addition, the nanoparticle were exposed to lipid bilayers and the mass change measured using a quartz crystal microbalance (QCM). This allowed us to look at the interaction of the negatively charged nanoparticles with lipid bilayers with different degrees of lipid tail saturation. The validity of using QCM mass change data to study the interaction of nanoparticle material at the solid/liquid interface has been demonstrated by the work of Xu *et al.*.[19] They demonstrated that QCM data for both laponite and Ludox show strong adsorption on poly(diallyldimethylammonium chloride) (PDADMAC) surfaces and that QCM showed larger frequency shifts for Ludox compared to laponite at all concentrations.

Although Lolicato *et al.* used molecular dynamics (MD) simulations to study the interaction between cationic gold nanoparticle and lipid bilayers consisting of distearoylphosphatidylcholine above their gel-to-fluid transition temperature, T_m, of 55 °C,[20] there is a general lack of information on the effect of temperature on the interaction of lipid layers with nanoparticles both above and below their gel-to-fluid phase transition and this was investigated for DPPC lipid by determining possible mass changes of a lipid bilayer deposited on the quartz crystal.

Experimental methods

Lipid model membranes

To evaluate the possible effects of exposure to functionalised nanoparticles on lipid model membranes the following lipids were studied (Figure 1): DOPC, DPPC, POPC, and POPG.

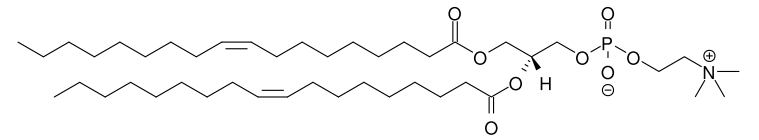

(a) DOPC

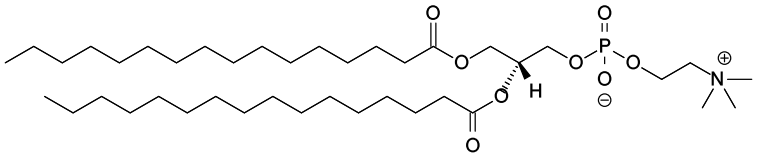

(b) DPPC

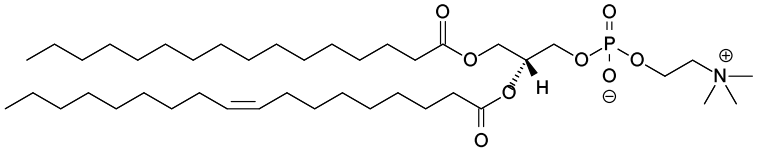

(c) POPC

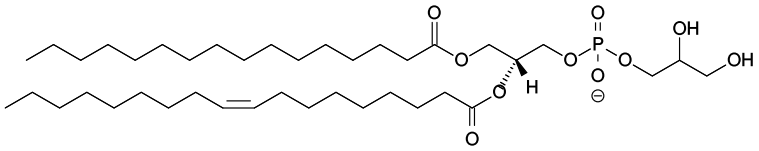

(d) POPG

Figure 1: The lipids used in this study: (a) DOPC, (b) DPPC, (c) POPC and (d) POPG. The lipids DPPC, DOPC and POPC are zwitterionic at physiological pH, whereas POPG carries a net negative charge.

Synthesis of citrate capped gold nanoparticles

Synthesis of the gold nanoparticles followed the method developed by Turkevich *et al.* and refined by Frens.[21,22] This method involves the reaction of hot gold(III) chloride solution with sodium citrate. The citrate acts as a reducing agent, causing the formation of gold atoms in solution according to the reaction:

$$\mathrm{Au^{3+}(aq) + 3\,e^{-} \longrightarrow Au^{0}(s)} \tag{1}$$

The gold atoms nucleate and form the gold nanoparticles. The citrate stabilises the

nanoparticles by binding to the surface and preventing further binding of the nuclei to form larger particles. The citrate capping gives the gold nanoparticles a negative surface charge. This surface charge causes the nanoparticles to repel each other in solution, making the nanoparticle solution very stable following synthesis. The nanoparticles synthesised for this study showed no signs of aggregation after one month.

A 1 mM gold(III) chloride solution was heated with constant stirring until boiling. Sodium citrate was added to give a 1:40 molar ratio of gold to citrate and the mixture kept at boiling point until the solution turned a deep red colour indicative of the production of gold nanoparticles. The nanoparticles were sized using dynamic light scattering (DLS) and had a measured Z-average hydrodynamic diameter of (18 ± 1) nm and polydispersity of 1.10 % as measured using dynamic light scattering (DLS). The concentration of gold in the nanoparticle solution formed from this method was $0.20\,\mathrm{mg\,ml^{-1}}$. The upper limit of particles per ml is 3.24×10^{12}, assuming 100 % conversion of the gold into nanoparticles of this size.

To prepare smaller diameter nanoparticles, the molar ratio of gold(III) chloride to sodium citrate used was 1:80. The reaction vessel was placed in cold water as soon as the characteristic red colour appeared to prevent further growth of the nanoparticles. The higher molar ratio of citrate to gold(III) chloride resulted in smaller measured diameter nanoparticles. This was due to the greater number of citrate molecules being available to cap and prevent further growth of the nanoparticles before they could get any larger. The measured Z-average hydrodynamic diameters of the nanoparticles were (9 ± 1) nm with polydispersity 2.60 % The upper limit of particles per ml is 2.35×10^{13}, assuming 100 % conversion of the gold into nanoparticles of this size.

CTAB functionalised gold nanoparticles.

CTAB is a quaternary ammonium surfactant that is used in the synthesis of positively charged nanoparticles.[23–25] The headgroup of the CTAB molecule carries a positive charge (Figure 2).

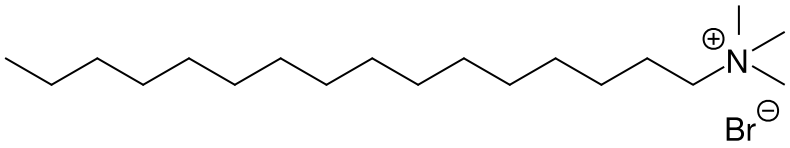

Figure 2: Molecular structure of cetyltrimethylammonium bromide (CTAB) used in the functionalisation of citrate capped gold nanoparticles.

Lim *et al.* propose a possible mechanism for the stabilisation of citrate capped nanoparticles that involves the CTAB molecules forming a bilayer of the surface of the nanoparticle.[23] The positively charged heads of the CTAB molecules are attracted to the negatively charged citrate capping with another layer of CTAB molecules forming the second leaflet of the bilayer (Figure 3). This bilayer stabilises the nanoparticles against aggregation due the the repulsive effects of the outer charged heads as well as giving the nanoparticles a positive surface charge.

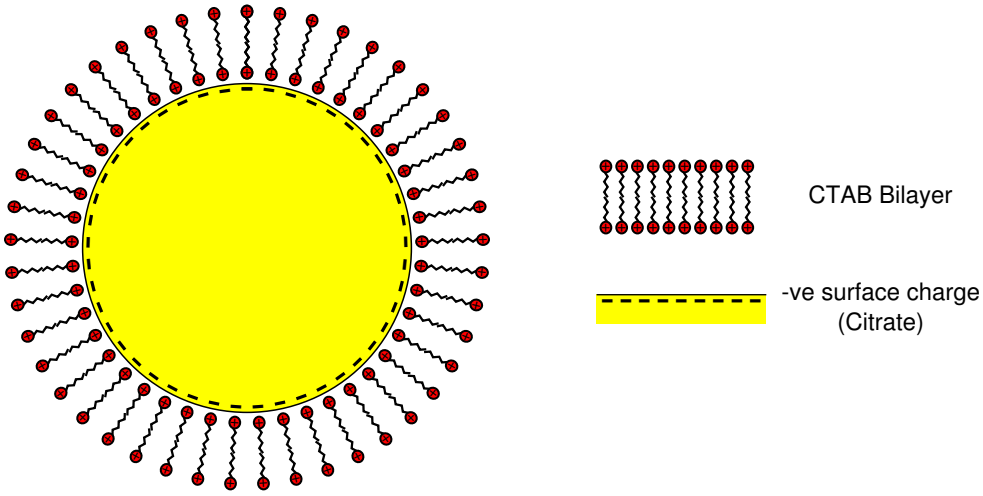

Figure 3: Possible method by which CTAB stabilises gold nanoparticles and imparts a positive charge to their surface. The positively charged heads are attracted to the negative charges of the citrate capping and a second layer of CTAB deposits forming a bilayer on the surface of the nanoparticle. This bilayer also gives the surface of the nanoparticle an overall positive charge. Schematic not to scale.

Gold seeds were prepared as follows. A 20 ml solution of 0.25 mM gold(III) chloride and 0.25 mM trisodium citrate was prepared. To this was added 0.60 ml of ice-cold 0.10 M sodium borohydride solution. On addition of the sodium borohydride, the solution immedi-

ately turned pink, indicating the formation of gold nanoparticle seeds by reduction of Au^+ according to the reactions:

$$NaBH_4 + 2\,H_2O \longrightarrow NaBO_2 + 8\,H^+ + 8\,e^- \tag{2}$$

$$8\,Au^+ + 8\,e^- \longrightarrow 8\,Au^0 \tag{3}$$

This solution was used within two hours.

A growth solution of 0.25 mM gold(III) chloride and 80 mM CTAB was heated until the solution turned a clear orange colour indicating the formation of a $AuCl_4^-$/CTAB complex according to the reaction:[26]

$$CH_3(CH_2)_{15}N^+(CH_3)_3 + AuCl_4^- \longrightarrow CH_3(CH_2)_{15}(CH_3)_3N{-}AuCl_4 \tag{4}$$

To 9 ml of this growth solution, 0.05 ml of 0.10 M ascorbic acid was added. While the solution was stirred vigorously, 1 ml of the seed solution was added. The ascorbic acid reduces the $AuCl_4^-$/CTAB complex to form Au^0 which deposits on the surface of the gold seeds and after ten minutes the solution turned a deep wine-red colour, indicating the formation of gold nanoparticles. To wash the nanoparticles, they were centrifuged at 11 000 g for 30 min, the supernatant discarded, and the resulting nanoparticle pellet re-dispersed in 10 ml of de-ionised water. This procedure was repeated four times to ensure removal of all excess CTAB. The concentration of gold in the nanoparticle solution formed from this method was $0.05\,mg\,ml^{-1}$. The washed nanoparticles were sized using DLS and had a measured Z-average hydrodynamic diameter of 17 nm and polydispersity of 2.10 %. The upper limit of particles per ml is 1.03×10^{12}, assuming 100 % conversion of the gold into nanoparticles of this size.

Changes to surface pressure/area isotherms.

The surface pressure, Π, is defined as:

$$\Pi = \gamma_{\mathrm{w}} - \gamma \tag{5}$$

where γ_{w} is the surface tension of the pure liquid subphase (usually water) and γ is the surface tension of the subphase with the monolayer of interest at the air-liquid interface. (The value of γ_{w} for pure water is $72.80\,\mathrm{mN\,m^{-1}}$ at $20\,^{\circ}\mathrm{C}$.[27])

By measuring the surface pressure of the air/water interface as a function of the monolayer area, the surface pressure/area isotherm can be obtained. A typical surface pressure/area isotherm for a lipid monolayer shows a rise in surface pressure as the area is reduced and the monolayer compressed. The presence of species such as nanoparticles will affect the interaction of the lipid molecules within the monolayer. This change in the interaction may affect how the lipid molecules pack together and this can cause changes in the observed surface-pressure/area isotherm from which information on the nature of the interaction can be deduced.

The Langmuir-Blodgett trough (102M model, Nima technologies, Coventry, UK) had a total surface area of $100\,\mathrm{cm^2}$. The Wilhelmy plate in this experiment consists of a rectangular piece of filter paper with a perimeter of 21.00 mm around the base (Whatman N°1, Maidstone, UK).

The trough was cleaned between each lipid deposition using water and chloroform before being filled with water (Millipore Milli-Q, $18\,\mathrm{M\Omega\,cm}$).

Using a Hamilton syringe, 6 µl of $1\,\mathrm{mg\,ml^{-1}}$ POPC (Avanti Polar Lipids, Alabaster, AL) in chloroform (Sigma-Aldrich, ACS reagent, ≥99.80 %, stabilised with ethanol) was deposited onto the surface of the subphase and the chloroform was allowed to evaporate. The temperature of the subphase was $(22 \pm 1)\,^{\circ}\mathrm{C}$.

For measuring the effect of the nanoparticles on the lipid monolayer, a 1 ml solution

of the 9 nm citrate capped gold nanoparticles was injected under the lipid monolayer and allowed to stabilise for 15 min before compressing the barriers. Following measurement of the surface pressure/area isotherm, the barriers were re-opened and a further 1 ml solution of citrate capped gold nanoparticles was injected under the monolayer and allowed to stabilise for 15 min before re-measuring the surface pressure/area isotherm by closing the barriers. This process was repeated once more, giving a total of three repeats of surface pressure/area isotherm measurements, each following exposure to 1 ml citrate capped gold nanoparticles.

Following removal of the subphase the trough was cleaned and 6 µl of 1 mg ml^{-1} solution of POPG (Avanti Polar Lipids, Alabaster, AL) in chloroform was deposited on a de-ionised water subphase and allowed to form a monolayer. A 1 ml volume of citrate capped gold nanoparticles was injected under the lipid monolayer and allowed to stabilise for 15 min before compressing the barriers. As with the POPC monolayer, this process was repeated a further two times to give a total of three repeats of the surface pressure/area isotherm for POPG. Both these procedures were repeated for 1 ml volumes of seed grown CTAB capped 17 nm nanoparticles.

Quartz crystal microbalance

Piezoelectric quartz crystal microbalances respond to the adsorption of materials on their surfaces by a change in their characteristic oscillating frequency.[28] The attachment of a film of mass, Δm, to the surface of the quartz crystal results in a decrease of the crystal's resonant frequency, Δf. If the change in mass, Δm, is small, then the relationship between Δf and Δm is linear and follows the Sauerbrey equation:

$$\Delta f = -\frac{f_n}{n}\frac{m_f}{m_q} = -f_0\frac{m_f}{m_q} \tag{6}$$

where f_o is the fundamental frequency of the quartz crystal, f_n is the natural oscillation frequency of the crystal at overtone number n, m_f is the mass per unit area of the film and

m_q is the mass per unit area of the quartz crystal itself.[5,29] By depositing a lipid bilayer on the surface of a quartz crystal balance and measuring any possible mass change as the quartz crystal/lipid system is exposed to nanoparticles in solution, it is possible to determine the factors that will affect the rate and extent of nanoparticle interaction with the lipid bilayer.

Two additional equations are relevant in the selection of the fundamental frequency of the quartz crystal used. The mass sensitivity, C, of the QCM crystal is inversely proportional to the square of the fundamental frequency:

$$C \propto \frac{1}{f_o^2} \tag{7}$$

Therefore, the higher the fundamental frequency, the greater the sensitivity to mass changes. However, the higher the fundamental frequency of the crystal, the thinner it must be manufactured and consequently the more fragile it will be. Also, higher frequency measurements will result in a corresponding increase in noise resulting in higher measurement uncertainty.

The fundamental frequency of the crystal used in this study is 10 MHz as this provides the most acceptable compromise of the factors given above. The sensing depth, δ, is inversely proportional to the square root of the frequency of the crystal:

$$\delta \propto \frac{1}{\sqrt{f_o}} \tag{8}$$

For a quartz crystal operating at a fundamental frequency of 10 MHz, the sensing depth is ≈180 nm. This is well in excess of the thickness expected for a lipid bilayer and nanoparticle adsorbed onto the crystal surface.

For this study, the QCM device used for measuring the interaction of gold nanoparticles with a deposited bilayer was the commercially available OpenQCM device, `www.openqcm.com` The method for depositing the lipid bilayer was described by Tabaei *et al.*, and Hohner *et al.* and is known as the solvent assisted lipid bilayer method (SALB).[30,31] It involves the gradual

replacement of the organic solvent in which the lipid is dissolved by an aqueous buffer within the same flow cell as the quartz crystal. As the aqueous fraction increases, a continuous lipid bilayer deposits on the surface of the quartz crystal's gold electrode.[31] Deposition of a DOPC bilayer using this method gave an average frequency drop of (-98.8 ± 13.9) Hz, which, based on the Sauerbrey equation, corresponds to 437 ng cm^{-2} for the hydrated bilayer, in agreement with the theoretical value proposed by Zwang et al.[32]

All lipids were supplied by Avanti Polar Lipids, Alabaster, AL. The lipid solutions were prepared as 0.50 mg ml^{-1} in propan-2-ol. For the aqueous buffer, a 10 mM Tris/150 mM NaCl buffer with a pH of 7.50 was used. The solutions were passed over the crystal surface using a peristaltic pump at a flow rate of 40 µl min^{-1}. Initially, 1 ml of Tris buffer was introduced into the quartz crystal flow cell and the frequency measured. This frequency was taken as the frequency of a quartz crystal under liquid without an adsorbed bilayer. A further 1 ml volume of pure propan-2-ol was injected into the flow cell to prevent premature interaction of the lipid/propan-2-ol solution with the aqueous buffer. The lipid solution, 1 ml, then used to fill the quartz crystal flow cell. Tris buffer was again pumped into the cell at a rate of 40 µl/ min to slowly increase the fraction of aqueous buffer to propan-2-ol. The volume of Tris buffer was increased until all propan-2-ol was flushed from the cell. The change in frequency of the crystal was measured during all changes of solution. The lipid bilayers were deposited at 22.50 °C and, in the case of DPPC only, at 45.00 °C. The latter temperature is above the gel-to-fluid transition temperature, T_m, of 41.40 °C for DPPC. Three repeats were carried out for 9 nm and 18 nm citrate capped gold nanoparticles (0.20 mg ml^{-1}) and the 17 nm CTAB capped gold nanoparticles (0.05 mg ml^{-1}). For each of the three solutions no dilution was carried out. The volume of nanoparticle containing solution was 1 ml in all repeats. The temperature of the solutions passing over the crystal was measured by a thermistor within the QCM flow cell. The temperature of the lipid bilayer was controlled by placing the QCM device, peristaltic pump and flow circuitry within a temperature-controlled oven. After the nanoparticle solution had passed through the flow cell, a 2 ml volume of Tris

buffer was introduced.

Results and Discussion

Lipid monolayer isotherms

Changes to the surface pressure/area isotherms of the lipids POPC and POPG were measured after exposure to both citrate capped and CTAB capped gold nanoparticles using a Langmuir-Blodgett trough. No increase in the surface pressure with decreasing surface area was observed in control experiments where the nanoparticles were injected into pure de-ionised water.

Surface pressure/area isotherms are shown for POPC and POPG lipid exposed to increasing quantities of citrate capped gold nanoparticles (Figure 4). The monolayer surface pressure/area isotherm shifts to higher molecular area on exposure to increasing amounts of nanoparticles. If the gold nanoparticles become included into the lipid monolayer, we would expect to see the monolayer surface pressure/area isotherm shift to higher molecular areas due to the reduction in total surface area available to the lipid molecules. If the nanoparticles were to become coated with lipid and subsequently leave the monolayer, the loss of lipid would result in a shift of the surface pressure/area isotherm to lower molecular areas. Both plots show a shift to higher molecular areas. However, the surface pressure/area isotherms for POPG plots are not shifted to higher molecular areas as much as those of POPC. The shifts in the isotherms to higher molecular area suggest that as the monolayer is exposed to increasing amounts of the citrate capped nanoparticles, they undergo inclusion into the monolayer and that they remain associated with the monolayer as it is compressed.

The plots of the difference in area versus surface pressure for both monolayers suggest a saturation effect as the concentration of nanoparticles increases. Up to approximately $12\,\mathrm{mN\,m^{-1}}$, there is no change in the compression modulus for POPC or POPG monolayers with or without nanoparticles. Above $12\,\mathrm{mN\,m^{-1}}$, the change in the compression modulus

could possibly be accounted for by a buckling of the monolayer.

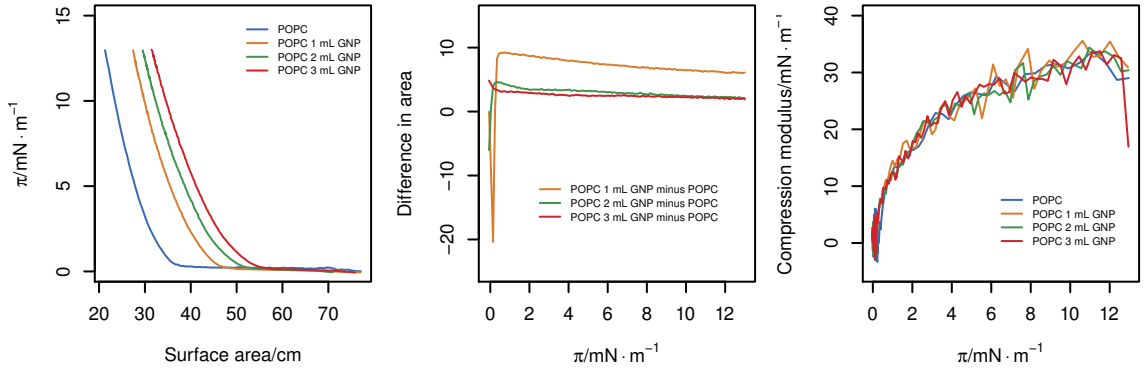

(a)

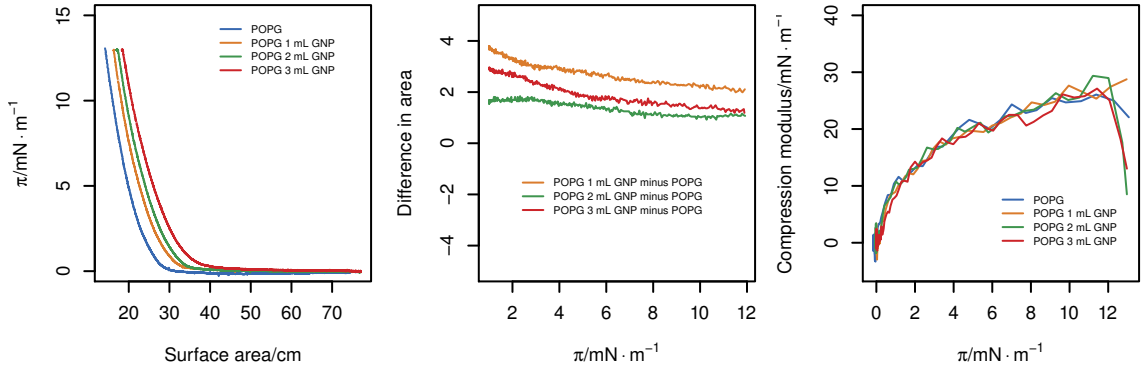

(b)

Figure 4: Surface pressure/area isotherms, difference in area and compression moduli, given by compression modulus, $K = -A\left(\frac{\partial \pi}{\partial A}\right)$, for (a) POPC and (b) POPG lipid monolayers exposed to citrate capped gold nanoparticles. The shift in the surface pressure/area isotherms to higher molecular areas following exposure to increasing amounts of nanoparticles in the subphase suggest that the nanoparticles undergo inclusion into the monolayer.

Surface pressure/area isotherms are shown for POPC and POPG lipid exposed to increasing quantities of CTAB capped gold nanoparticles (Figure 5). The shift in the surface pressure/area isotherms to higher molecular areas following exposure to increasing amounts of nanoparticles in the subphase suggest that, as was the case with the citrate capped nanoparticles, the nanoparticles undergo inclusion into the monolayer and that they remain within the monolayer. However, the surface pressure/area isotherms are shifted to higher molecular areas more than the same monolayers exposed to citrate capped nanoparticles. Also, for the POPG lipid, the shift in the surface pressure/area isotherm to higher molecular

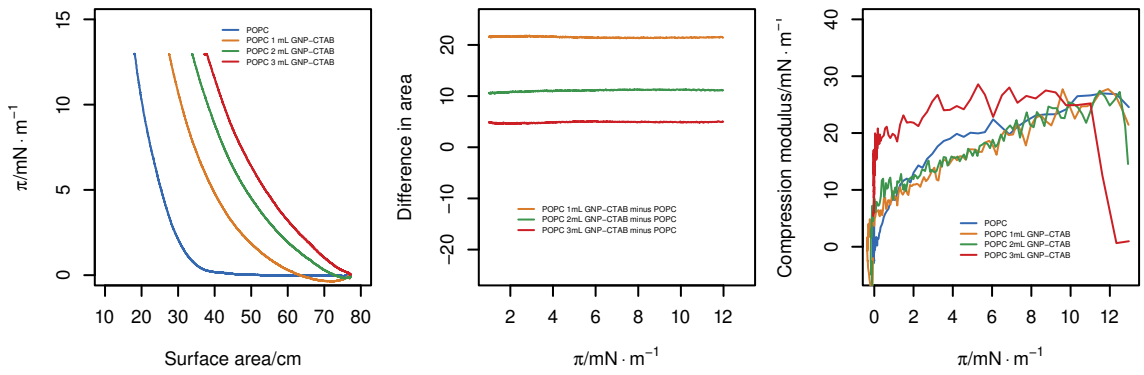

(a)

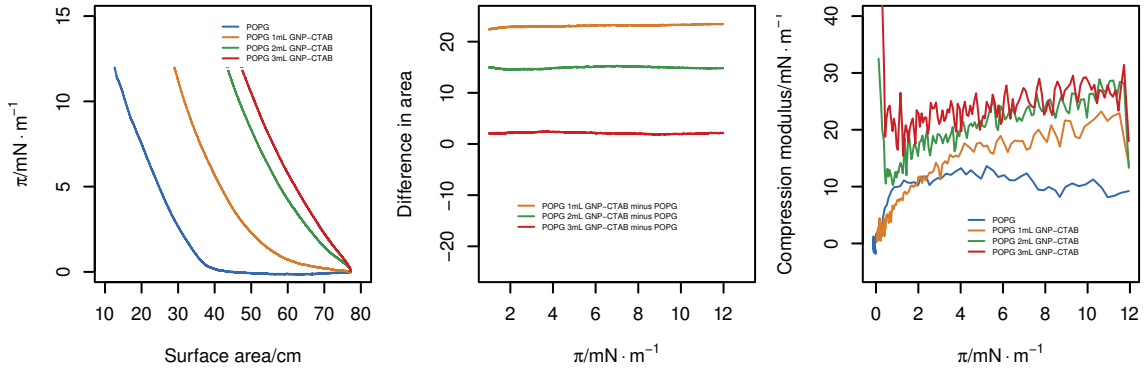

(b)

Figure 5: Surface pressure/area isotherms, difference in area and compression moduli, given by compression modulus, $K = -A\left(\frac{\partial \pi}{\partial A}\right)$, for (a) POPC and (b) POPG lipid monolayers exposed to CTAB capped gold nanoparticles. The shift in the surface pressure/area isotherms to higher molecular areas following exposure to increasing amounts of nanoparticles in the subphase suggest that, as with the citrate capped gold nanoparticles, the nanoparticles undergo inclusion into the monolayer.

area is greater than for the POPC monolayers whereas the shift observed when the negatively charged citrate gold nanoparticles were injected under POPG monolayers was less than for POPC monolayers.

For the POPC monolayer, the number of lipid molecules at the surface was 4.75×10^{15}. The increase in area per molecule corresponds to 6.55×10^{12} Å^2 for the whole POPC monolayer. The minimum number of citrate capped nanoparticles that would need to be included into the monolayer to account for this area increase is 2.52×10^{10}, giving a ratio of lipid molecules to nanoparticles of 1.90×10^5:1. For the CTAB capped nanoparticles, the number needed to account for an area increase of 1.08×10^{13} Å^2 is 4.89×10^{10}, giving a ratio of lipid

molecules to nanoparticles of 9.70×10^4:1.

For the POPG monolayer, the number of lipid molecules at the surface was 4.69×10^{15}. The increase in area per molecule upon the addition of the citrate capped particles corresponds to 1.77×10^{12} Å^2 for the whole POPG monolayer. The number of citrate capped nanoparticles that would need to be included into the monolayer to account for this area increase is 8.81×10^9, giving a ratio of lipid molecules to nanoparticles of 6.90×10^5:1. For the CTAB capped nanoparticles, the number needed to account for an area increase of 1.45×10^{13} Å^2 is 6.55×10^{10}, giving a ratio of lipid molecules to nanoparticles of 7.20×10^4:1.

The results demonstrate that the nature of the functionalisation of the nanoparticles affects the association with, or more likely degree of penetration of, the nanoparticles into the lipid monolayer; however, in all cases a shift in the surface pressure/area isotherm to larger areas was observed, indicating at least some inclusion of the particles in the lipid layer, as described by Guzmán *et al.*. This supports the work of Pfeiffer *et al.*, who showed enhanced interaction of positively charged gold nanoparticles with POPG lipids compared to POPC.[14]

The least change is observed for the negatively charged citrate coated particles and the negatively charged POPG monolayers, suggesting the anionic headgroups of the POPG lipids partially repel the anionic surface charge of the citrate capped nanoparticles limiting the degree of inclusion, but not to the extent that no interaction is seen. For both lipid monolayers, POPC and POPG, the positively charged CTAB coated nanoparticles cause a larger shift in the surface pressure/area isotherm, indicating more inclusion, than was the case for the negatively charged citrate capped nanoparticles but care must be taken not to attribute this purely to the charge difference as the CTAB coated particles have a very different structure to the citrate capped ones.

As expected, the greater effect is seen for the positively charged CTAB coated particles with the negatively charged POPG monolayers than the Zwitterionic POPC monolayers, which supports the observation of Goodman *et al.*, who observed that gold nanoparticles

coated with a positively charged surfactant species caused more lysis of vesicles composed of mixed PC/PG lipids than those containing only PC lipids.[33]

Quartz crystal microbalance

Zwang *et al.* give a mass of 431.80 ng cm^{-2} for a DOPC bilayer and its associated hydration layer.[32] The quoted sensitivity of the 10 MHz OpenQCM crystal is 4.42×10^{-9} g Hz^{-1} cm^{-2}, giving a theoretical frequency drop of 97.70 Hz. Deposition of a DOPC bilayer using the SALB method gives an average frequency drop of (-98.8 ± 13.9) Hz, which is in agreement with the theoretical value (Figure 6).

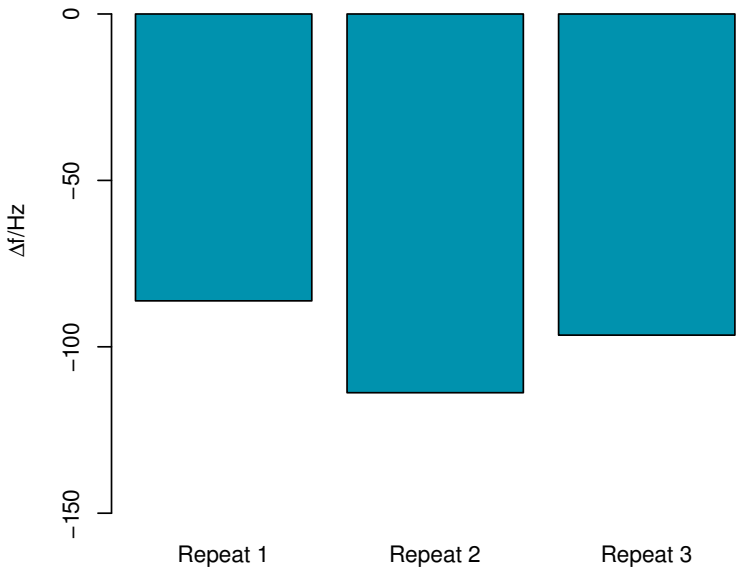

Figure 6: Repeats of the frequency response of a 10 MHz OpenQCM quartz crystal following deposition of a DOPC lipid bilayer using the SALB protocol. The measured frequency drops from the were −86.20 Hz (Repeat 1), −113.80 Hz (Repeat 2) and −96.50 Hz (Repeat 3). The mean frequency drop was (-98.8 ± 13.9) Hz, in close agreement with the theoretical frequency drop of 97.70 Hz expected for a QCM crystal with a sensitivity of 4.42×10^{-9} g Hz^{-1} cm^{-2}.

A bare quartz crystal microbalance exposed to 18 nm diameter gold nanoparticles showed a small decrease in frequency due to adsorption of low levels of the nanoparticles onto the crystal (Figure 7).

A decrease in oscillating frequency of the quartz crystal microbalance with adsorbed lipid bilayer was observed for all three lipids (DPPC, DOPC and POPC) studied when exposed to 18 nm and 9 nm diameter gold nanoparticles (Figures 8–14). The decrease in frequency is indicative of an increase in mass due to the nanoparticles being adsorbed onto the surface of the crystal.

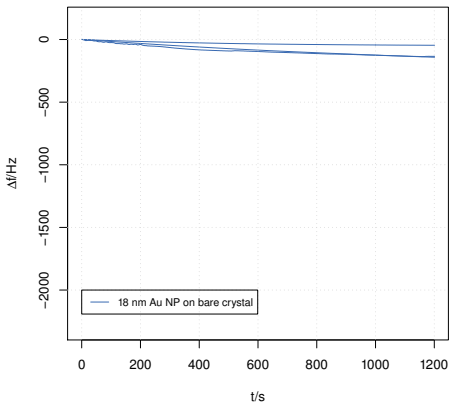

Figure 7: Plot of frequency change, $\Delta f = f - f_0$ (where f_0 is the fundamental frequency of the crystal and f is the measured frequency), as a function of time, t, for a bare crystal exposed to 18 nm Au NPs. Three repeats were carried out with a clean crystal and fresh nanoparticle solution used for each run.

At first glance this appears to be in direct contrast to the findings of Bailey *et al.* who also used QCM-D to monitor changes when fluid phosphocholine lipid bilayers were exposed to citrate capped gold nanoparticles of 2, 5, 10 and 40 nm.[5] In all cases, the authors report a very slight increase in the frequency, i.e. a small loss of mass (presumably lipid) from the bilayer. However, the nanoparticle solutions used by the authors were two orders of magnitude more dilute, in terms of particles per ml, than the solutions used here and, as the authors suggest, they were likely working below the level required to observe a measurable decrease in signal, based on an approximate value for the lipid bilayer/water distribution

coefficient of nanoparticles (450 L kg^{-1} lipid for tannic acid capped gold particles).[34] Using the same distribution coefficient and the higher number concentration of nanoparticles used in this work we would expect to see a measurable drop in frequency, indeed we actually observe a larger drop in frequency suggesting the distribution coefficients of citrate capped nanoparticles between water and fluid lipid bilayers is about 30 times greater than that for tannic acid capped particles, or ≈13 500 l kg^{-1}, although the difference is not so large that Bailey *et al.* would have expected to see a measurable drop in frequency under their conditions. Thus it appears our results are in agreement with Bailey *et al.*, citrate capped particles do distribute between the bulk water and supported fluid bilayers.

Frequency changes for the quartz crystal coated with the lipid bilayers, DPPC, DOPC and POPC were plotted with respect to time for both nanoparticle sizes 18 nm and 9 nm (Figures 8 – 14). The lipid bilayers were exposed to gold nanoparticles for 20 min at a temperature of 22.50 °C. Frequency changes for DPPC bilayers exposed to 18 nm citrate capped gold nanoparticles at 45.00 °C, which is above their gel-to-fluid transition temperature, T_m, of 41.40 °C, were also plotted (Figure 8).

The rate and extent of adsorption of 18 nm gold nanoparticles by a DPPC bilayer below its gel-to-fluid transition temperature, T_m, of 41.40 °C was much less than that of the bilayer above T_m. Mecke *et al.* have observed that polymer coated particles interaction only with the fluid phase of DMPC lipid bilayers.[35] bilayer above its gel-to-fluid transition temperature. This suggests that some degree of molecular mobility within the bilayer is necessary for interaction between the lipid molecules and the nanoparticles. Bailey *et al.* studied the effect of exposure of phosphocholine bilayers to 40 nm gold nanoparticles and suggest that particle interaction with the bilayer involves the engulfment of the nanoparticle by lipid molecules.[5] They suggest that the bending modulus, κ, is a factor in the negative free energy change between the nanoparticle coated with lipid state and the initial state of the planar bilayer and un-adsorbed nanoparticle. Adsorption of a nanoparticle onto a lipid bilayer would be more energetically favourable if the engulfment of the nanoparticle was facilitated by a greater

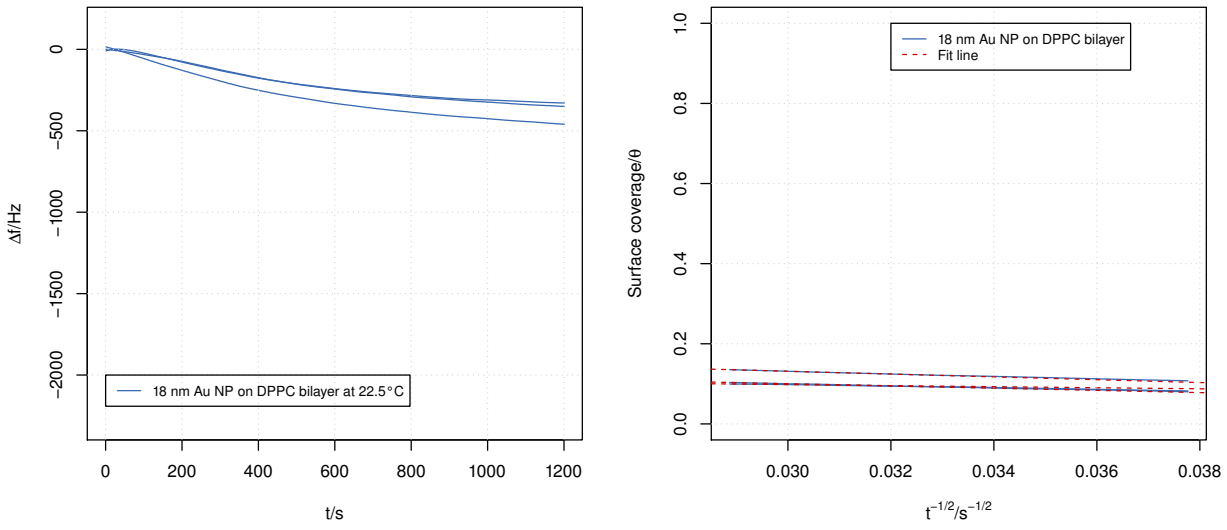

(a) (b)

Figure 8: Plot of frequency change, $\Delta f = f - f_0$ (where f_0 is the fundamental frequency of the crystal and f is the measured frequency), as a function of time, t, for a DPPC bilayer (a) below its gel-to-fluid transition temperature, T_m, of 41.40 °C exposed to 18 nm citrate capped Au NPs and (b) a plot of surface coverage, θ, with respect to $t^{-1/2}$. Plot (a) shows a decrease in frequency due to deposition of nanoparticles. However, the drop in frequency for a DPPC bilayer below its transition temperature is less than that of a DPPC bilayer above its transition temperature (Figure 9). This shows that the uptake of nanoparticles of a DPPC bilayer is reduced if the bilayer is below the gel-to-fluid transition temperature. Plot (b) fitted lines show a linear relationship of θ versus $t^{-1/2}$ at large t (small $t^{-1/2}$) which indicates that the system shows random sequential adsorption (RSA) kinetics and a saturation effect on the adsorption process as the surface of the bilayer becomes covered in nanoparticles. Three repeats were carried out with a fresh lipid layer and fresh nanoparticle solution used for each run.

degree of movement of lipid molecules within the bilayer.

A possible model for the adsorption of nanoparticles onto a lipid bilayer is the random sequential adsorption (RSA) model.[36] This model assumes that the nanoparticles are adsorbed at random locations on the bilayer surface and that there is no lateral movement of the particle after adsorption. In the RSA model, as the concentration of nanoparticles at the bilayer surface increases there will be a reduction in the rate of change of mass with respect to time as less and less of the bilayer surface is available for further nanoparticle adsorption.

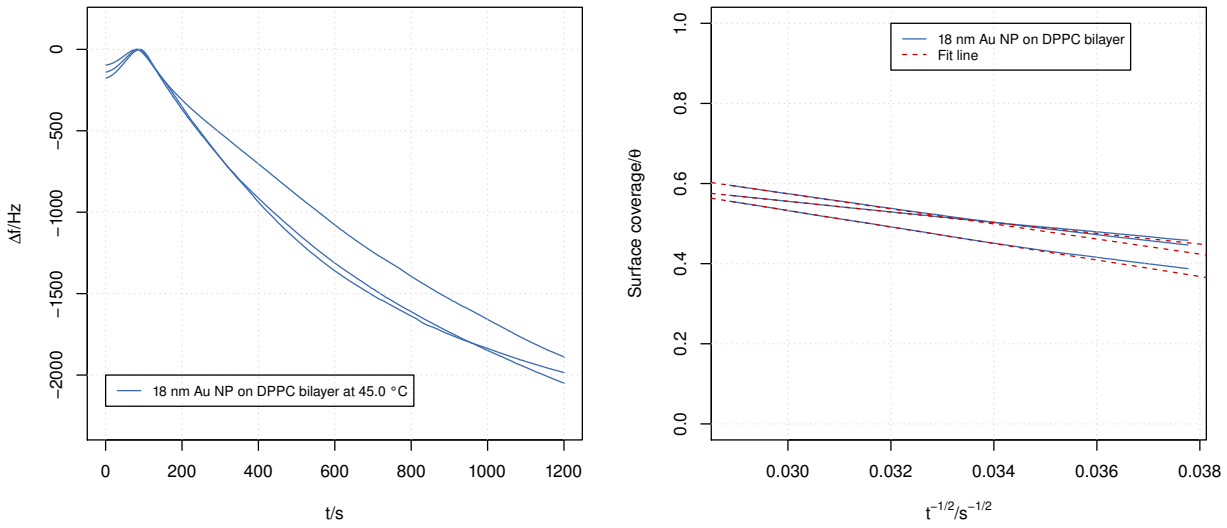

(a) (b)

Figure 9: Plot of frequency change, $\Delta f = f - f_0$ (where f_0 is the fundamental frequency of the crystal and f is the measured frequency), as a function of time, t, for a DPPC bilayer (a) above its gel-to-fluid transition temperature, T_m, of 41.40 °C exposed to 18 nm citrate capped Au NPs and (b) a plot of surface coverage, θ, with respect to $t^{-1/2}$. Plot (a) shows a decrease in frequency due to deposition of nanoparticles. The drop in frequency for a DPPC bilayer below its transition temperature is greater than that of a DPPC bilayer below its transition temperature (Figure 8). Plot (b) fitted lines show a linear relationship of θ versus $t^{-1/2}$ at large t (small $t^{-1/2}$) which indicates that the system shows random sequential adsorption (RSA) kinetics and a saturation effect on the adsorption process as the surface of the bilayer becomes covered in nanoparticles. Three repeats were carried out with a fresh lipid layer and fresh nanoparticle solution used for each run.

Plotting the decrease in frequency, and therefore the concentration of nanoparticles at the bilayer surface, shows an initial rapid change in frequency with respect to time which decreases as nanoparticles continue to be introduced into the system. As the surface coverage, θ, is proportional to the concentration of nanoparticles at the bilayer, the plots of frequency against time show that there is a limiting saturation value, $\theta(\infty)$, where theoretically the whole of the bilayer surface is covered with nanoparticles. For systems for which the RSA model is valid, it is accepted that the surface coverage approaches a jamming limit that follows a power law relationship[36]

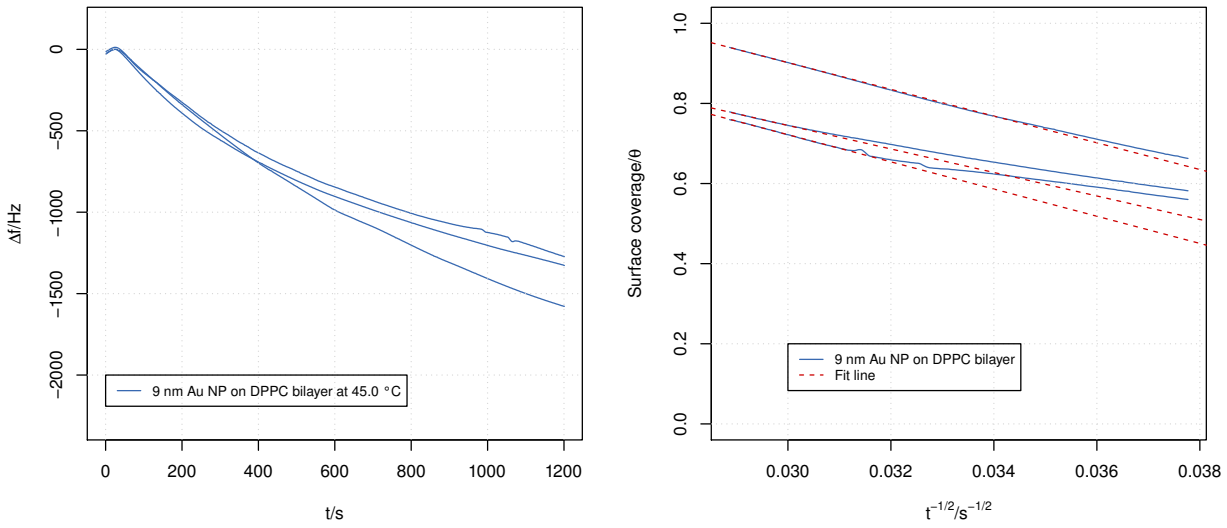

(a) (b)

Figure 10: Plot of frequency change, $\Delta f = f - f_0$ (where f_0 is the fundamental frequency of the crystal and f is the measured frequency), as a function of time, t, for a DPPC bilayer exposed to 9 nm citrate capped gold nanoparticles at 45.00 °C which is above its gel-to-fluid transition temperature, T_m, of 41.40 °C and (b) a plot of surface coverage, θ, with respect to $t^{-1/2}$. Three repeats were carried out with a fresh lipid layer and fresh nanoparticle solution used for each run.

$$\theta(\infty) - \theta(t) \approx t^{-\frac{1}{d}} \tag{9}$$

where d is dependent on the number of translational degrees of freedom for the particle. For spherical nanoparticles on a surface, the number of degrees of freedom is 2. If the RSA model is valid for the adsorption of nanoparticles on lipid bilayers, a plot of surface coverage, θ, with respect to $t^{-1/2}$ would show a linear relationship at large t. Surface coverage, θ, with respect to $t^{-1/2}$ for lipid bilayers exposed to 18 nm citrate capped gold nanoparticles were plotted (Figure 8 (b) to Figure 14 (b)). The fitted lines show a linear relationship of θ versus $t^{-1/2}$ at large t (small $t^{-1/2}$) which indicates that the system shows random sequential adsorption (RSA) kinetics and a saturation effect on the adsorption process as the surface of the bilayer becomes covered in nanoparticles. Surface coverages, θ, at $t = \infty$ for all lipids

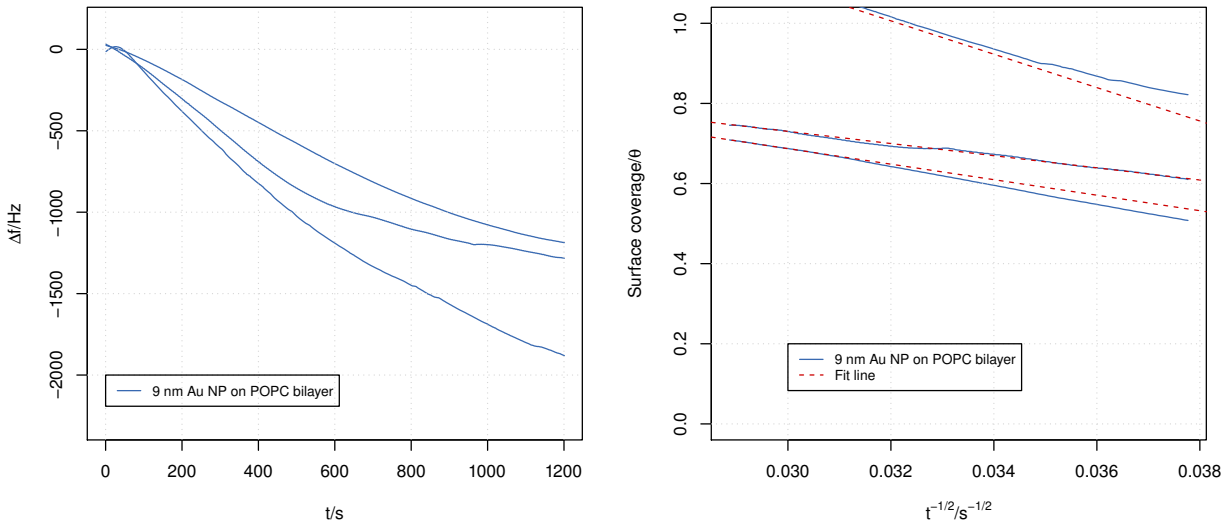

(a) (b)

Figure 11: Plot of frequency change, $\Delta f = f - f_0$ (where f_0 is the fundamental frequency of the crystal and f is the measured frequency), as a function of time, t, for a POPC bilayer exposed to 9 nm citrate capped gold nanoparticles at 22.50 °C and (b) a plot of surface coverage, θ, with respect to $t^{-1/2}$. Three repeats were carried out with a fresh lipid layer and fresh nanoparticle solution used for each run.

exposed to 9 nm and 18 nm citrate capped Au NPs are given in Table 1.

Frequency changes for DPPC bilayers exposed to 17 nm CTAB capped gold nanoparticles were measured. Exposure to the CTAB capped nanoparticles resulted in a reduction in the oscillation frequency of the QCM, indicating that instead of particles depositing on the bilayer, a loss of mass had occurred. This suggests that the lipid bilayers are removed by the interaction of the lipid with the nanoparticles flowing over them. The frequency of the crystal reverted to the frequency of a bare gold surface, indicating that the CTAB capped nanoparticles had stripped the bilayer.

The complete removal of the DPPC bilayer by the CTAB coated particles at temperatures below the gel-fluid phase transition temperature was not expected. Tatur *et al.* have looked at similar system and found no evidence of interaction of their smaller but similarly structured positively charged gold nanoparticles with a DSPC bilayer below the transition

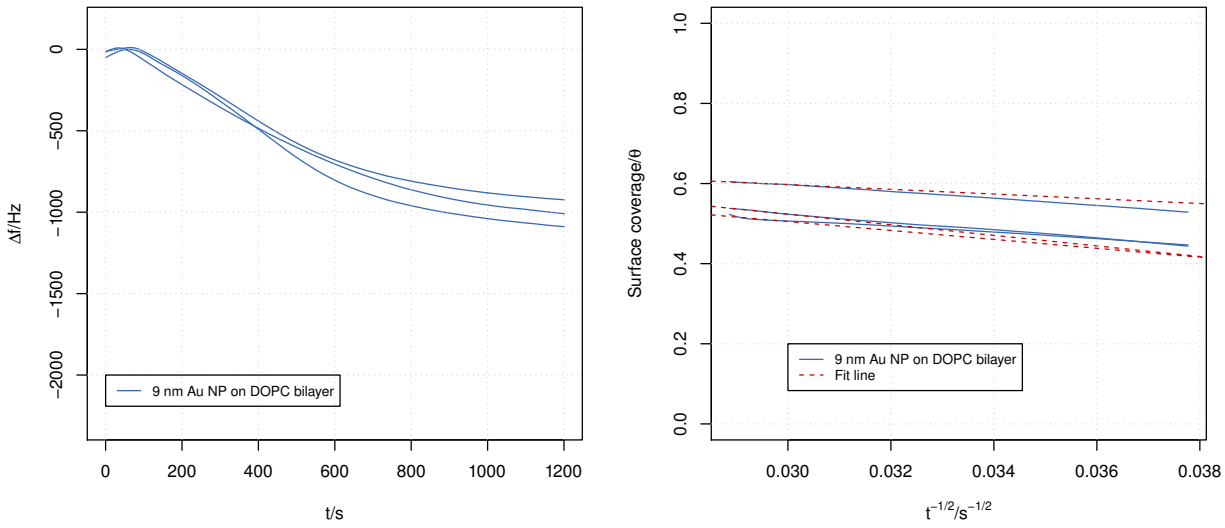

(a) (b)

Figure 12: Plot of frequency change, $\Delta f = f - f_0$ (where f_0 is the fundamental frequency of the crystal and f is the measured frequency), as a function of time, t, for a DOPC bilayer exposed to 9 nm citrate capped gold nanoparticles at 22.50 °C and (b) a plot of surface coverage, θ, with respect to $t^{-1/2}$. Three repeats were carried out with a fresh lipid layer and fresh nanoparticle solution used for each run.

temperature for the lipid, however they did observe complete removal of the bilayer when exposed to the cationic particles above the transition temperature.[37] The particles used by Tatur *et al.*, were capped with N,N,N-trimethyl(11-mercaptoundecyl) ammonium groups, and so, although very similar in structure to the CTAB capped particles used in this work, the particles used in the current work have a longer hydrophobic tail section (C16 compared to C11). In addition the DSPC bilayer of Tatur *et al.*, had two more carbon atoms in each tail compared to the DPPC we used. Thus whilst the hydrophobic tail region of our particles patched the tails of the lipid bilayer, in the case of Tatur *et al.*, the tail of the particles was significantly shorter than the tail of the bilayer, which may indicate whilst removal of the bilayer was only feasible at higher temperatures. Also, Tatur *et al.* used solutions with a gold concentration of 0.01 mg ml^{-1} gold compared with a concentration of 0.05 mg ml^{-1} gold concentration of the solutions used in this study.

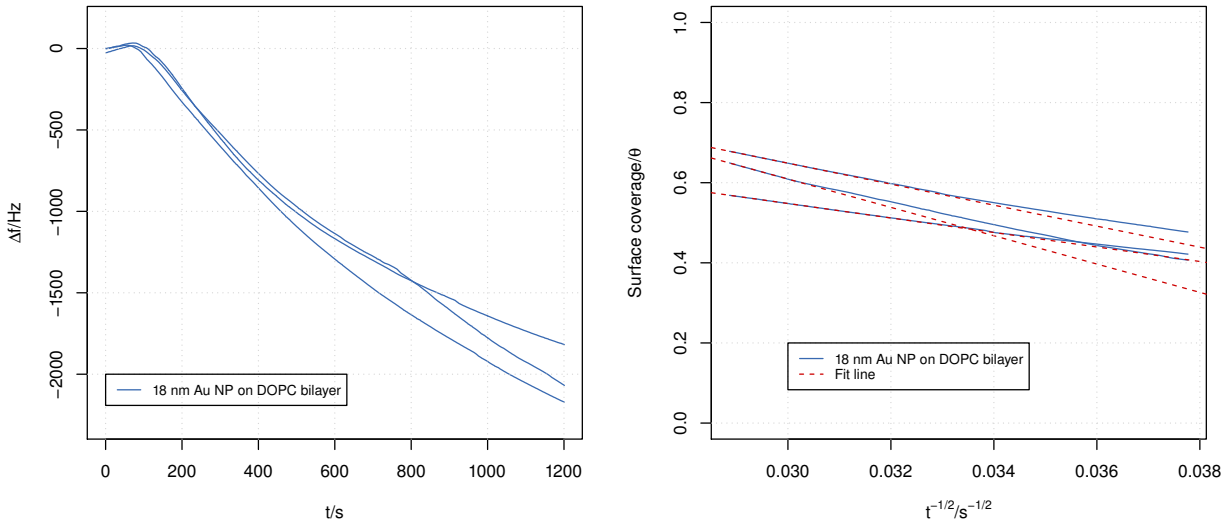

(a) (b)

Figure 13: Plot of frequency change, $\Delta f = f - f_0$ (where f_0 is the fundamental frequency of the crystal and f is the measured frequency), as a function of time, t, for a DOPC bilayer exposed to 18 nm citrate capped gold nanoparticles at 22.50 °C and (b) a plot of surface coverage, θ, with respect to $t^{-1/2}$. Three repeats were carried out with a fresh lipid layer and fresh nanoparticle solution used for each run.

Table 1: Table of surface coverage, θ, with respect to $t = \infty$ for all lipids exposed to 9 nm and 18 nm citrate capped Au NPs.

Surface	Temperature/°C	Surface coverage, θ, at $t = \infty$, mean value from 3 repeats (range).	
		9 nm citrate capped Au NP	18 nm citrate capped Au NP
Gold	22.5	0.08 (0.03–0.18)	0.06 (0.02–0.10)
DPPC bilayer	22.5	—	0.19 (0.14–0.24)
DPPC bilayer	45.0	1.76 (1.63–1.90)	1.08 (0.96–1.15)
POPC	22.5	1.60 (1.18–2.34)	1.15 (1.05–1.31)
DOPC	22.5	0.84 (0.77–0.92)	1.40 (1.09–1.67)

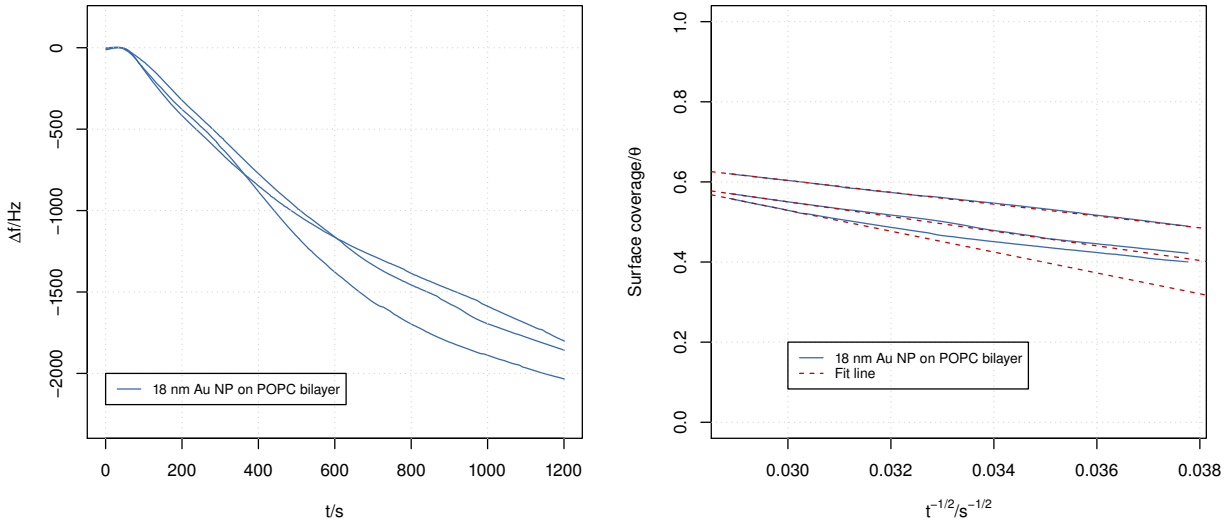

(a) (b)

Figure 14: Plot of frequency change, $\Delta f = f - f_0$ (where f_0 is the fundamental frequency of the crystal and f is the measured frequency), as a function of time, t, for a POPC bilayer exposed to 18 nm citrate capped gold nanoparticles at 22.50 °C and (b) a plot of surface coverage, θ, with respect to $t^{-1/2}$. Three repeats were carried out with a fresh lipid layer and fresh nanoparticle solution used for each run.

QCM dissipation monitoring

The frequency change and dissipation of a DOPC bilayer exposed to different concentrations of 18.20 nm citrate capped gold nanoparticles were plotted (Figure 15). The solutions of nanoparticles were of concentrations 0.15 %, 0.10 % and 0.05 % of mass of gold nanoparticles in solution.

There is an initial change in the energy dissipation on the initial introduction of the nanoparticle solution (<20 sec) which can be attributed to the density changes due to the Tris buffer within the cell being replaced by the nanoparticle solution. However, as the mass on the surface of the quartz crystal increases due to the deposition of the nanoparticles, there is no significant change in the energy dissipation from the crystal. This suggests that the viscosity of the lipid bilayer is not greatly affected by the deposition of the gold nanoparticles. This would suggest that interaction with the nanoparticles does not greatly affect the structure of the bilayer.

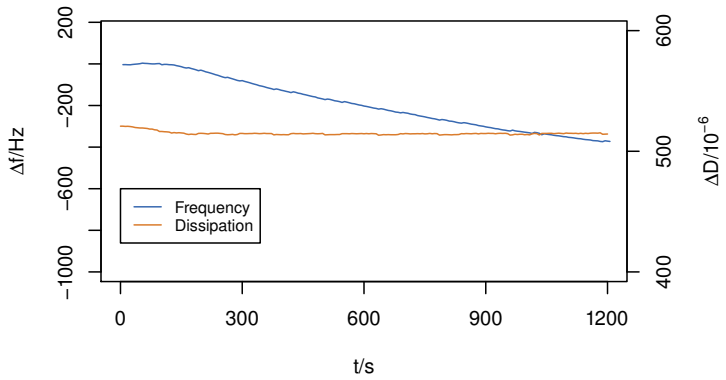

(a) 0.05 % mass of gold in solution.

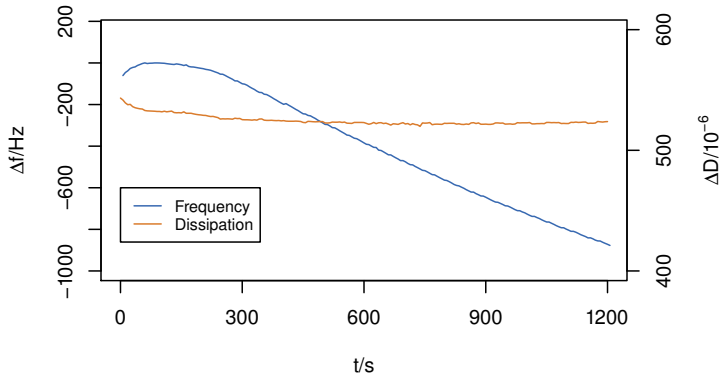

(b) 0.10 % mass of gold in solution.

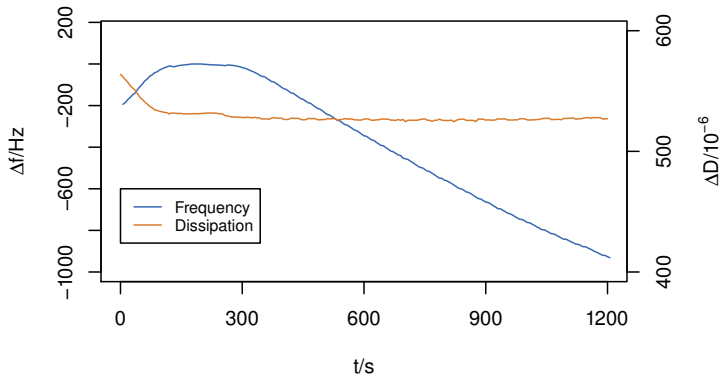

(c) 0.15 % mass of gold in solution.

Figure 15: Plots of frequency change and dissipation of DOPC bilayer exposed to different concentrations of citrate capped gold nanoparticles. The plots show that the dissipation of the lipid bilayer during deposition of the gold nanoparticles does not change significantly. This suggests that the viscosity of the lipid bilayer is not greatly affected by the deposition of the gold nanoparticles.

Conclusions

Changes to the surface pressure/area isotherms of the lipids POPC and POPG were measured after exposure to both citrate capped and CTAB capped gold nanoparticles using a Langmuir-Blodgett trough. Exposure of both POPC and POPG monolayers to anionic citrate capped particles showed a shift in the surface pressure/area isotherms to higher molecular areas which suggests that the nanoparticles undergo inclusion into the monolayer. The shift was less pronounced in the case of the negatively charged POPG monolayers than POPC, the data suggesting the number of particles per lipid for POPG was only 0 27 times what it was for POPC for the same number of particles injected. Exposure of POPC and POPG monolayers to positively charged CTAB capped nanoparticles also showed a shift in the surface pressure/area isotherms to higher molecular areas, again suggesting that the nanoparticles undergo inclusion into the monolayer. In the case of the cationic particles the particle to lipid ratio was greater with the negatively charged POPG monolayer than with the POPC monolayer. These results show that the interaction of nanoparticle materials with lipid monolayers is dependent on both the charge on the lipid layer and the charge of the capping material used on the nanoparticle. Previous work by others have shown that, at least for neutral particles, the hydrophilicity of the particle of the particle is also important.[38]

In order to examine the differing uptake of citrate capped particles on lipid bilayers with different tail group compositions a series of QCM measurements were undertaken. It was found that the uptake of particles to a DPPC bilayer below its phase transition temperature was extremely low, whereas extensive uptake was observed above the phase transition temperature, extrapolation suggesting complete coverage would occur at infinite exposure time. The uptake of particles to DPPC bilayers above the phase transition temperature was similar to that of the fluid phase bilayers of DOPC and POPC. The results suggest that the increase in the molecular mobility, and subsequent change in the bending modulus, κ, of the bilayer above the phase is required for particle uptake.

Dissipation monitoring of a DOPC bilayer exposed to three concentrations by mass of

gold nanoparticles was carried out. The dissipation of the bilayer did not show an appreciable change even at high lipid coverage. Little change in dissipation indicates that the viscosity of the DOPC bilayer was not greatly affected by the deposition of the gold nanoparticles. A possible reason for this is that the interaction with the nanoparticles does not greatly affect the structure of the bilayer. If lipid molecules were being removed at an appreciable level, this loss, and the replacement of the lipid molecules by water molecules within the bilayer, could be expected to reduce viscosity of the bilayer and this would be indicated by a change in dissipation.

Bailey *et al.* carried out similar dissipation monitoring of a L-α-phosphatidylcholine bilayer exposed to 10 nm a nd 40 nm gold nanoparticles.[5] They observed negligible dissipation changes in the bilayer following exposure to the gold nan oparticles. They concluded that this implies that the lipid bilayer on the QCM crystal can be treated as a rigid film and that the frequency changes obse rved are a direct result of the mass changes due to adsorption of nanoparticles.

References

(1) Hu, X.; Zhang, Y.; Ding, T.; Liu, J.; Zhao, H. Multifunctional gold nanoparticles: a novel nanomaterial for various medical applications and biological activities. *Frontiers in Bioengineering and Biotechnology* **2020**, *8*, 990.

(2) Contini, C.; Schneemilch, M.; Gaisford, S.; Quirke, N. Nanoparticle-membrane interactions. *Journal of Experimental Nanoscience* **2018**, *13*, 62–81.

(3) Sohlenkamp, C.; Geiger, O. Bacterial membrane lipids: diversity in structures and pathways.

(4) Bakshi, M. S.; Zhao, L.; Smith, R.; Possmayer, F.; Petersen, N. O. Metal nanoparticle

pollutants interfere with pulmonary surfactant function in vitro. *Biophysical Journal* **2008**, *94*, 855–868.

(5) Bailey, C. M.; Kamaloo, E.; Waterman, K. L.; Wang, K. F.; Nagarajan, R.; Camesano, T. A. Size dependence of gold nanoparticle interactions with a supported lipid bilayer: a QCM-D study. *Biophysical Chemistry* **2015**, *203*, 51–61.

(6) Guzmán, E.; Liggieri, L.; Santini, E.; Ferrari, M.; Ravera, F. Influence of silica nanoparticles on thermodynamic and structural properties of DPPC–palmitic acid Langmuir monolayers. *Colloids and Surfaces A: Physiochemical and Engineering Aspects* **2012**, *413*, 280–287.

(7) Guzmán, E.; Santini, E.; Ferrari, M.; Liggieri, L.; Ravera, F. Interaction of Particles with Langmuir Monolayers of 1,2-Dipalmitoyl-Sn-Glycero-3-Phosphocholine: A Matter of Chemistry? *Coatings* **2020**, *10*.

(8) Guzmán, E.; Liggieri, L.; Santini, E.; Ferrari, M.; Ravera, F. DPPC-DOPC langmuir monolayers modified by hydrophilic silica nanoparticles: phase behaviour, structure and rheology. *Colloids and Surfaces A - Physiochemical and engineering aspects* **2012**, *413*, 174–183.

(9) Orsi, D.; Guzmán, E.; Liggieri, L.; Ravera, F.; Ruta, B.; Chushkin, Y.; Rimoldi, T.; L., C. 2D dynamical arrest transition in a mixed nanoparticle-phospholipid layer studied in real and momentum spaces. *Scientific reports* **2015**, *5*, 17930.

(10) Guzmán, E.; Liggieri, L.; Santini, E.; Ferrari, M.; Ravera, F. Mixed DPPC–cholesterol Langmuir monolayers in presence of hydrophilic silica nanoparticles. *Colloids and Surfaces B: Biointerfaces* **2013**, *105*, 284–293.

(11) Guzmán, E.; Ferrari, M.; Santini, E.; Liggieri, L.; Ravera, F. Effect of silica nanoparticles on the interfacial properties of a canonical lipid mixture. *Colloids and Surfaces B: Biointerfaces* **2015**, *136*, 971–980.

(12) Van Lehn, R. C.; Alexander-Katz, A. Structure of Mixed-Monolayer-Protected Nanoparticles in Aqueous Salt Solution from Atomistic Molecular Dynamics Simulations. *The Journal of Physical Chemistry C* **2013**, *117*, 20104–20115.

(13) Van Lehn, R. C.; Atukorale, P. U.; Carney, R. P.; Yang, Y.-S.; Stellacci, F.; Irvine, D. J.; Alexander-Katz, A. Effect of particle diameter and surface composition on the spontaneous fusion of monolayer-protected gold nanoparticles with lipid bilayers. *Nano Letters* **2013**, *13*, 4060–4067.

(14) Pfeiffer, T.; De Nicola, A.; Montis, C.; Carlà, F.; van der Vegt, N. F. A.; Berti, D.; Milano, G. Nanoparticles at Biomimetic Interfaces: Combined Experimental and Simulation Study on Charged Gold Nanoparticles/Lipid Bilayer Interfaces. *The Journal of Physical Chemistry Lett* **2019**, *10*, 129–137.

(15) Schaeublin, N. M.; Braydich-Stolle, L. K.; Schrand, A. M.; Miller, J. M.; Hutchison, J.; Schlager, J. J.; Hussain, S. M. Surface charge of gold nanoparticles mediates mechanism of toxicity. *Nanoscale* **2011**, *3*, 410–420.

(16) Torrano, A.; Pereira, A.; Oliveira, O.; Barros-Timmons, A. Probing the interaction of oppositely charged gold nanoparticles with DPPG and DPPC Langmuir monolayers as cell membrane models. *Colloids Surf B Biointerfaces* **2013**,

(17) Hu, P.; Qian, W.; Liu, B.; Pichan, C.; Chen, Z. Molecular interactions between gold nanoparticles and model cell membranes: a study of nanoparticle surface charge effect. *The Journal of Physical Chemistry C* **2016**, *120(39)*, 22718–22729.

(18) Canepa, E.; Salassi, S.; Simonelli, F.; Ferrando, R.; Rolandi, R.; Lambruschini, C.; Canepa, F.; Dante, S.; Relini, A.; Rossi, G. Non-disruptive uptake of anionic and cationic gold nanoparticles in neutral zwitterionic membranes. *Scientific Reports* **2021**, *11(1256)*.

(19) Xu, D.; Hodges, C.; Ding, Y.; Biggs, S.; Brooker, A.; York, D. A QCM Study on the Adsorption of Colloidal Laponite at the Solid/Liquid Interface. *Langmuir* **2010**, *26*, 8366–72.

(20) Lolicato, F.; Joly, L.; Martinez-Seara, H.; Fragneto, G.; Scoppola, E.; Baldelli Bombelli, F.; Vattulainen, I.; Akola, J.; Maccarini, M. The Role of Temperature and Lipid Charge on Intake/Uptake of Cationic Gold Nanoparticles into Lipid Bilayers. *Small* **2019**, *15*.

(21) Turkevich, J.; Stevenson, P. C.; Hillier, J. A study of the nucleation and growth processes in the synthesis of colloidal gold. *Discussions of the Faraday Society* **1951**, *11*, 55–75.

(22) Frens, G. Particle-size and sol stability in metal colloids. *Kolloid-Zeitschrift and Zeitschrift für Polymere* **1972**, *250*, 736.

(23) Lim, J.; Lee, N. E.; Lee, E.; Yoon, S. Surface modification of citrate capped gold nanoparticles using CTAB micelles. *Bulletin of the Korean Chemical Society* **2014**, *35*, 2567–2569.

(24) Jana, N. R.; Gearheart, L.; Murphy, C. J. Seeding growth for size control of 5-40 nm diameter gold nanoparticles. *Langmuir* **2001**, *17*, 6782–6786.

(25) Faham, R.; Samadi, A.; Abolhasani, J. CTAB-capped gold nanoparticles as a new probe for spectrophotometric determination of heparin. *Journal of Applied Spectroscopy* **2017**, *84*, 425–430.

(26) Khan, Z.; Singh, T.; Hussain, J. I.; Hashmi, A. A. Au(III)-CTAB reduction by ascorbic acid: Preparation and characterization of gold nanoparticles. *Colloids and Surfaces B-Biointerfaces* **2013**, *104*, 11–17.

(27) Davies, J.; Rideal, E. *Interfacial Phenomena*; Academic Press, New York and London, 1963.

(28) King, W. Piezoelectric sorption detector. *Analytical Chemistry* **1964**, *36*, 1735–1739.

(29) Sauerbrey, G. Verwendung von Schwingquarzen zur Wägung dünner Schichten und zur Mikrowägung. *Zeitschrift für Physik* **1959**, *155*, 206–222.

(30) Tabaei, S. R.; Choi, J. H.; Zan, G. H.; Zhdanov, V. P.; Cho, N. J. Solvent-assisted lipid bilayer formation on silicon dioxide and gold. *Langmuir* **2014**, *30*, 10363–10373.

(31) Hohner, A. O.; David, M. P. C.; Raedler, J. O. Controlled solvent-exchange deposition of phospholipid membranes onto solid surfaces. *Biointerphases* **2010**, *5*, 1–8.

(32) Zwang, T. J.; Fletcher, W. R.; Lane, T. J.; Johal, M. S. Quantification of the layer of hydration of a supported lipid bilayer. *Langmuir* **2010**, *26*, 4598–4601.

(33) Goodman, C. M.; McCusker, C. D.; Yilmaz, T.; M., R. V. Toxicity of gold nanoparticles functionalized with cationic and anionic side chains. *Bioconjugate Chemistry* **2004**, *15(4)*, 897–900.

(34) Hou, W. C.; Moghadam, B. Y.; Gorredor, C.; Westerhoff, P.; Posner, J. D. Distribution of functionalized gold nanoparticles between water and lipid bilayers as model cell membranes. *Environmental Science & Technology* **2012**, *46(3)*, 1869–1876.

(35) Mecke, A.; Lee, D. K.; Ramamoorthy, A.; Orr, B. G.; Holl, M. M. B. Synthetic and natural polycationic polymer nanoparticles interact selectively with fluid-phase domains of DMPC lipid bilayers. *Langmuir* **2005**, *21(19)*, 8588–8590.

(36) Feder, J. Random sequential adsorption. *Journal of Theoretical Biology* **1980**, *87*, 237–254.

(37) Tatur, S.; Maccarini, M.; Barker, R.; Nelson, A.; Fragneto, G. Effect of functionalized gold nanoparticles on floating lipid bilayers. *Langmuir* **2013**, *29(22)*, 6606–6614.

(38) Guzmán, E.; Santini, E.; Ferrari, M.; Liggieri, L.; Ravera, F. Effect of the incorporation of nanosized titanium dioxide on the interfacial properties of 1,2-dipalmitoyl-sn-glycerol-3-phosphocholine langmuir monolayers. *Langmuir* **2017**, *33*, 10715–10725.